

# Full Impedance Cardiography Measurement Device Using Raspberry PI3 and System-on-Chip Biomedical Instrumentation Solutions

Abdelakram Hafid<sup>1</sup>, Sara Benouar, Malika Kedir-Talha, Farhad Abtahi<sup>1</sup>, Mokhtar Attari,  
and Fernando Seoane, *Senior Member, IEEE*

**Abstract**—Impedance cardiography (ICG) is a noninvasive method for monitoring cardiac dynamics using electrical bioimpedance (EBI) measurements. Since its appearance more than 40 years ago, ICG has been used for assessing hemodynamic parameters. This paper presents a measurement system based on two System on Chip (SoC) solutions and Raspberry PI, implementing both a full three-lead ECG recorder and an impedance cardiograph, for educational and research development purposes. Raspberry PI is a platform supporting Do-It-Yourself project and education applications across the world. The development is part of Biosignal PI, an open hardware platform focusing in quick prototyping of physiological measurement instrumentation. The SoC used for sensing cardiac biopotential is the ADAS1000, and for the EBI measurement is the AD5933. The recordings were wirelessly transmitted through Bluetooth to a PC, where the waveforms were displayed, and hemodynamic parameters such as heart rate, stroke volume, ejection time and cardiac output were extracted from the ICG and ECG recordings. These results show how Raspberry PI can be used for quick prototyping using relatively widely available and affordable components, for

supporting developers in research and engineering education. The design and development documents will be available on [www.BiosignalPI.com](http://www.BiosignalPI.com), for open access under a Non Commercial-Share A like 4.0 International License.

**Index Terms**—AD5933, ADAS1000, bioimpedance, biosignal PI, biomedical instrumentation, cardiac monitoring, personalized healthcare, portable ECG, ICG, Raspberry PI3.

## I. INTRODUCTION

A ESTIMATED 17.5 million deaths per year are attributed to cardiac diseases. According to WHO [1], people with cardiovascular diseases (CVD)s such as hypertension, diabetes, hyperlipidemia or presenting high risk for CVD require an early and pertinent diagnosis to receive the best treatment [2]. In most of those cases, access to costly and complex instrumentation, is of paramount importance for an accurate diagnostic test, often only available at central hospitals.

Electrical bioimpedance (EBI) is one way of measurement that has been used for several decades for various applications; utilizing different measurement techniques e.g., segmental, total body [3], single frequency [4], spectroscopy [5], multichannel [6], single channel [7] and tomography [8]. One commonly used modality of the EBI technology is impedance plethysmography [9] and its most common application has been impedance cardiography (ICG). Using a single channel with single frequency continuously, the ICG was introduced as a non-invasive method for the assessment of the mechanical function of the heart and a commercial version were developed in 1967, for the National Aeronautics and Space Administration, NASA [10].

Since then, analysis of the ICG waveform has been used for the assessment of certain hemodynamic parameters describing the mechanical function of the heart like the cardiac output (CO), stroke volume (SV) and systolic time intervals, e.g., left ventricular ejection time (LVET), pre-ejection period (PEP), systolic time ratio (STR) [11]–[13]. A detailed introduction about ICG is available in Appendix I. Currently ICG measurements are found useful in number of conditions according to the United States department of health and human services (USHHS) [14]:

- Differentiation of cardiogenic from pulmonary causes of acute dyspnea.

Manuscript received May 23, 2017; revised September 25, 2017 and November 15, 2017; accepted December 8, 2017. Date of publication December 15, 2017; date of current version October 15, 2018. This work has been supported by The Ministère de l'Enseignement Supérieur et de la Recherche Scientifique, Algerian Government and The research group Textile and Wearable Sensing for p-Health Solutions, University of Borås. (*Corresponding author: Abdelakram Hafid.*)

A. Hafid and S. Benouar are with the Laboratory of Instrumentation, University of Sciences and Technology Houari Boumediene, Algiers 16111, Algeria, and also with the Department of Textile Technology, University of Borås, Borås 503 32, Sweden (e-mail: hafidakram@hotmail.com; sara\_benouar@hotmail.fr).

M. Kedir-Talha and M. Attari are with the Laboratory of Instrumentation, University of Sciences and Technology Houari Boumediene, Algiers 16111, Algeria (e-mail: malikakedir@gmail.com; attari.mo@gmail.com).

F. Abtahi is with the Institute of Environmental Medicine, Karolinska Institute, Stockholm SE-171 77, Sweden, also with the KTH School of Technology and Health, Stockholm 141-52, Sweden, and also with the Department of Clinical Physiology, Karolinska University Hospital, Huddinge 141 86, Sweden (e-mail: farhad.abtahi@ki.se).

F. Seoane is with the Swedish School of Textiles, University of Borås, Borås 50190, Sweden, with the Department of Clinical Science, Intervention and Technology, Karolinska Institutet, Stockholm 14186, Sweden, and also with the Department of Biomedical Engineering, Karolinska University Hospital, Stockholm 14186, Sweden (e-mail: fernando.seoane@hb.se).

Digital Object Identifier 10.1109/JBHI.2017.2783949

- Optimization of atrioventricular (A/V) interval for patients with A/V sequential cardiac pacemakers.
- Monitoring of continuous inotropic therapy for patients with terminal congestive heart failure.
- Evaluation for rejection in patients with a heart transplant as a predetermined alternative to a myocardial biopsy.
- Optimization of fluid management in patients with congestive heart failure.

An ICG recording is obtained using a specific electrode configuration, the electrodes are placed on the surface of the upper torso, and the EBI is measured across the thorax with the 4-electrode measurement technique from the neck to the abdomen [15]. The variation of impedance ( $Z$ ) measured is noted  $\Delta Z$ , and it is mainly due to the cardiac activity. The ICG recording also produces the  $dZ/dt$  waveform, which is obtained from the first derivative of the  $\Delta Z$  signal. The ICG waveforms together with the recorded ECG have been used to calculate and assess the specific hemodynamics parameters mentioned above [11], [12].

Several commercial stationary and/or mobile ICG measurement instruments exist with different technical characteristics, such as: Nicromo (medis. Germany), physioflow (Manatec, France), BioZ ICG Monitor (cardiodynamics, USA), Mobile impedance cardiograph (Mindware Technologies, USA), ICON (Osypka Medical, Germany) [16], [17]. While some of these commercial devices can be applied in home care setting most of them are specifically targeting hospital clinical settings and all of them share that are based in proprietary technology and none of them are meant to be used for educational purposes nor supporting quick prototyping for developing novel p-health applications to third parties openly. In order to do that, the scientific community needs open access or open hardware solutions such as Gamma Cardio Soft (open ECG) [18] or Biosignal PI [19] which are open source projects meant to support the development of novel p-health applications.

P-health: Preventive, pervasive, and personalized healthcare monitoring is demanding the deployment of novel applications based in biomedical sensing technologies [20]–[23]. Advances in textile manufacturing and smart textiles has allowed new developments of wearable measurements systems targeting fitness, and even home-care but often they have been limited to biopotential recordings [24], [25]. Recently advances in microelectronics has produced SoC solutions for biopotential and bioimpedance measurements as the ADS1292R, ADS1298R (Texas Instruments, inc. Texas, US) and the ADAS 1000-1 (Analog Device, Inc. Massachusetts, US) that are allowing to measure thoracic bioimpedance in addition to ECG, the AFE4300 (Texas Instruments, inc. Texas, US) performing multi-frequency bioimpedance measurement for body composition and the AD5933 (Analog Device, Inc. Massachusetts, US) able to provide both continuously single frequency impedance measurement or spectroscopy impedance measurement.

Most of them have been successfully tested in several EBI applications [26]–[34]. Thus, we can confirm that their availability and accessibility has indeed, fostered research and development activities targeting p-health monitoring based in different embedded electronics wearable measurement systems or even patch technology [34]–[38].

Since the Raspberry Pi platform was introduced, projects have investigated its suitability for developing biomedical sensing systems [19], [39]. Raspberry PI is presented as a mini-computer of reduced size that offers the possibility of use in a wide variety of fields and applications, Biosignal PI is an interesting example based on Raspberry PI aimed to make available a flexible and affordable educational platform for biomedical engineering field. Unfortunately, as most of available examples, until now, its main focus has been biopotential recording applications.

Following the original goal of biosignal PI, in this paper a measurement system based in the same core is developed with an updated Raspberry PI3, implementing both a full 3-lead ECG recorder and an impedance cardiograph, combining two SoC solutions: the ADAS1000 for ECG recording and the AD5933 working in continuous EBI plethysmography sensing mode.

## II. SYSTEM OVERVIEW

The developed ICG recording device, named Z-RPI, includes a Raspberry PI3, an impedance calibration system, wireless communication, a power management circuit and LiPo battery as power supply and EBI an ECG SoC measurement modules.

The Z-RPI designed according to technical specification detailed in Appendix II.

### A. Raspberry PI 3

The version used in this instrument is the 3rd generation of the Raspberry Pi card, named Raspberry Pi 3B. It is based on a Broadcom BCM2837, 64-bit, ARMv8 quad-core Cortex A53 processor operating at 1.2 GHz. It includes 1 GB of RAM. In addition to a HDMI port that can be connected to a portable LCD display for graphical interface, four USB 2.0 ports that can be used with a variety of devices such as a keyboard or a mouse. 40 general-purpose input/output (GPIO) are providing I2C, SPI, UART and simple Inputs/Outputs. Bluetooth 4.1 module based on the BCM43438 chip that include both Bluetooth low energy mode and classic Bluetooth mode, Wi-Fi module and Ethernet Port are also integrated in the platform [40], [41].

The Raspberry PI3 requires a power supply with a nominal current of 2.5 A, 5 V. The central storage of the system is a Micro-SD memory card. Raspberry PI3 allows for a multitude of programming languages like Scratch, Python, C/C++, and others, making it very flexible for rapid developments [40].

Raspberry PI like Arduino or BeagleBone allows wired communication through several different buses like SPI and I<sup>2</sup>C but furthermore, Raspberry PI incorporates wireless capabilities like Bluetooth and Wi-Fi. Therefore, it is more complete and versatile platform for the intended goal.

The language chosen for programming the Z-RPI device was C programming language mainly using the libraries available for the Broadcom BCM2835 1.52 [42]. These libraries allow access to the GPIO pins, and define specific instruction and functions to use the I<sup>2</sup>C communication protocols. The Bluez library was used for implementing the wireless communication.

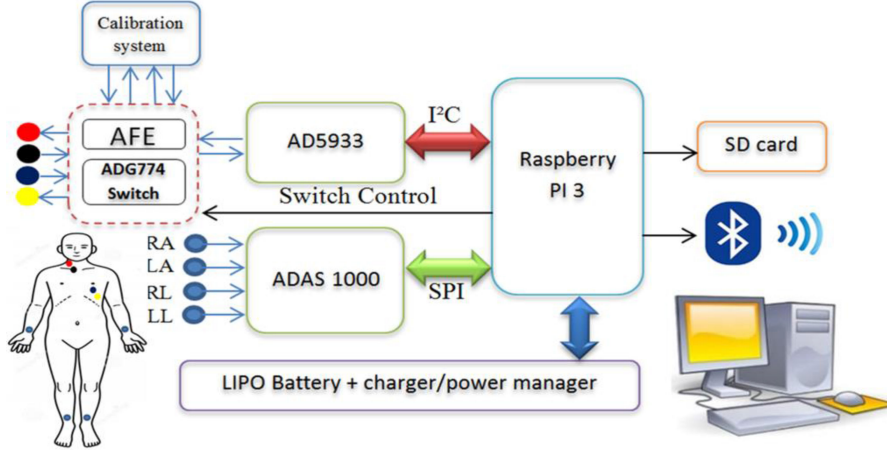


**Fig. 1.** Architecture of the system.

### B. Bioimpedance Measurement Unit

The SoC AD5933 impedance network analyzer manufactured by Analog Devices is the core of the EBI recording system. As such, the AD5933 performs amperometric impedance measurement between 2 terminals from  $1\text{ k}\Omega$  to approximately  $10\text{ M}\Omega$  in programmable intended frequency range from 1 kHz to 100 kHz according to manufacturer specifications [43], and upper frequency limit of 550 kHz have been reported [44], [45]. As a SoC, the AD5933 system equipped with an I<sup>2</sup>C buss has several advantages like low power consumption, and small size, but it is not suitable for performing EBI measurements in its standard configuration as detailed explained in [46], [47].

To enable the AD5933 for implementing EBI applications a specific analog-front-end (AFE) was introduced in [46], that among other limitations, it cancels the DC stimulation existing in the AD5933 enabling its use in humans by complying with electrical safety guidelines and improving measurement performance by implementing a 4-terminal technique, current driven voltametric impedance measurements adapted to impedance load systems between  $0\text{ }\Omega$  and  $1\text{ k}\Omega$  compatible with both segmental and full body EBI measurements.

### C. ECG Analogue Front-End module

The SoC ADAS1000 is a fully integrated ECG AFE manufactured by Analog Devices, designed to simplify the development of medical devices for cardiac activity applications [48]–[50]. This integrated Circuit (IC) significantly reduces the size and the number of components required for implementing an ECG acquisition system [51].

The ADAS1000 is a single IC that includes several ECG measurement options. It is built as a 5-electrode system for ECG signal acquisition, allowing performing 6-lead ECG studies. It includes impedance recording signal frequency 2-terminal port to measure respiratory movement.

The low power consumption, the programmable sample rate (up to 128 kHz), the programmable block filter, the ADC, the high SNR, and the SPI bus communication [51] ensure a high-

quality performance, as reported by [29] for ECG recordings, and makes the ADAS1000 a natural choice for our device.

### D. Calibration System

The AD5933 requires calibration before performing any EBI measurement. Generally this step is done manually, but to do the calibration steps automatically in the Z-RPI, the Analog Switch Multiplexer ADG774 circuit from Analog Devices is used. It is a monolithic CMOS device with four 2:1 multiplexer/demultiplexers with low power dissipation and a high switching speed device [52]. It provides the possibility to switch between the calibration stage and the measurement stage by programming two GPIO Raspberry PI3 pins.

In the Z-RPI device, the calibration is used with a configuration of 2R1C circuits, a resistor of  $150\text{ }\Omega$  0.1% in series with a capacitor of  $10\text{ nF}$  1%, both in parallel with a resistor of  $75\text{ }\Omega$  0.1% used to simulate the model of typical thorax impedance response [44].

### E. Wireless Communications

The Raspberry Pi3 allows for several means to communicate with another system or PC. For our device, Bluetooth 4.1 was chosen in its classic mode to implement the wireless communications.

The Z-RPI is configured to establish a wireless communication with a PC, implementing a Bluetooth RFCOMM protocol with socket communications [53] to transmit the samples acquired by the EBI and the ECG recorders.

## III. METHODS

### A. System Design and Operation

**Fig. 1** shows the block diagram of the Z-RPI, the Raspberry Pi3 represent the core of the device. It configures and performs measurements by ADAS1000 and AD5933, manages the switching between the measurement and calibration modes, stores the acquired data into Micro SD card and transfers them to the PC via the Bluetooth.

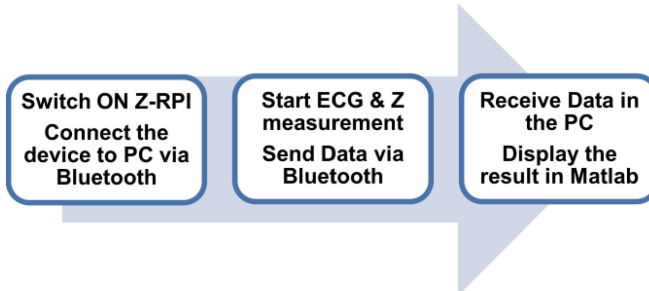


**Chart 1.** Operation and user manipulation of the Z-RPI.

**TABLE I**  
MEAN AND THE SD OF ANTHROPOMORPHIC DATA OF VOLUNTEERS

Gender	N	Height (cm)	Weight (kg)	Age (years)
Male	4	178 ± 4	73 ± 8	28 ± 8
Female	1	166	63	26

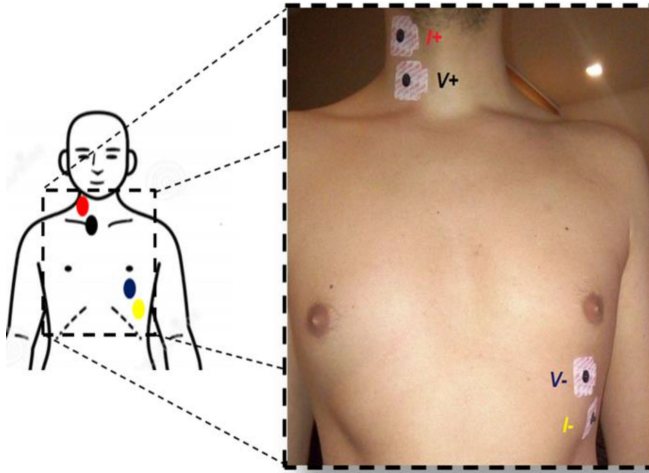


**Fig. 2.** Placement of electrodes for ICG measurement.

Chart 1 describes the functional sequence of operation for performing a measurement with the Z-RPI and its visualization on the computer.

### B. Experimental Measurement setup

After the functional measurement test described in Appendix III, the experimental evaluation was performed at the laboratory for Medical Textile-Electronics at the University of Borås, Sweden, on 5 healthy volunteers, see Table I. Prior to the measurements, all the subjects were properly informed and each of them signed the consent form according to the ethical approval 274-11 granted by the Regional Ethical Vetting Board in Gothenburg.

Fig. 2 shows the four 3M repositionable Ag/AgCl gel electrodes placed for performing the ICG recording according to the Sramek configuration [15]. Two electrodes are placed on the right lateral part of the neck, and two electrodes are placed

the left side of the thorax. The ECG electrodes were placed in wrist and ankles according to Einthoven triangle with a fourth electrode as right leg-driven.

When performing an ICG measurement using a tetrapolar configuration, the voltage sensing electrodes are the inner electrodes, marked with V, and the current injecting electrodes are the outer ones, indicated with I. ECG and ICG recording were obtained for at least 5 minutes while the subjects remained in setting position keeping a shallow breathing paced at 10 breaths per minute. The measurements are done using 90 cm shielded cables with 2.2 mm crocodile clips to attach the electrode.

### C. Measurement Data Analysis

The recorded thoracic measurement were processed and analyzed off-line on the PC using a customize program running MATLAB 2015 (The MathWorks, Inc. Massachusetts, US) scripts as presented in Appendix IV. The pre-processing and the analysis flow of the perform measurements is demonstrated in Chart 2.

**1) Heart Beat Detection:** The R peak and the Q point are extracted from the PQRST complex of the ECG signal by using the Pan and Tompkins algorithm which used to calculated heart rate and RR intervals in beat per minutes and milliseconds respectively. This algorithm has a simple implementation and an accurate performance [54]. The Q point is the minimum before the R peak, it was found at 40 ms before R [55].

**2) ICG Parameters:** The  $\Delta Z$  and  $dZ/dt$  signals obtained from the ICG recording were analyzed to obtain the following ICG parameters, see Table II. More detailed description of the  $dZ/dt$  signal with its characteristic points and hemodynamic parameters are given in Appendix I. The ICG parameters were calculated using mainly two ICG characteristic points (X and B point) and the R and Q point on the ECG, by applying a peak detector triggered by the synchronous R peak of the ECG to detect the E point in the R-R interval. Thus, the B point was calculated by using the standard zero crossing method at 15% response on the  $dZ/dt_{max}$  (E point) waveform [56]. Moreover the X point was determined as the minimum value of  $dZ/dt$  signal after the E point and before O point [57].

The ET, HR and PEP parameters were used to calculate SV, CO and STR (1), (2) and (3) respectively [12], [13].

$$SV = V_C \sqrt{\frac{dZ(t)/dt_{max}}{Z_0} ET} \quad (1)$$

$$CO = SV \times HR \quad (2)$$

$$STR = PEP/ET \quad (3)$$

Where  $V_C$  is the volume conductor constant equal to  $16 \text{ W}^{1.02}$  in  $\text{mL}$  and  $W$  is the weight expressed in  $\text{kg}$ ,  $dZ/dt_{max}$  is the peak of the first derivative of the transthoracic impedance variation in  $\Omega/\text{s}$ ,  $Z_0$  is the transthoracic base impedance in  $\Omega$ .

Due to the fact that the morphology of the ICG waveform is actually changing in morphology [58]–[61], such variability actually influence in the detection of the characteristic points and consequently calculation of the hemodynamic parameters. For assessing some-how the goodness of the ICG recordings, the

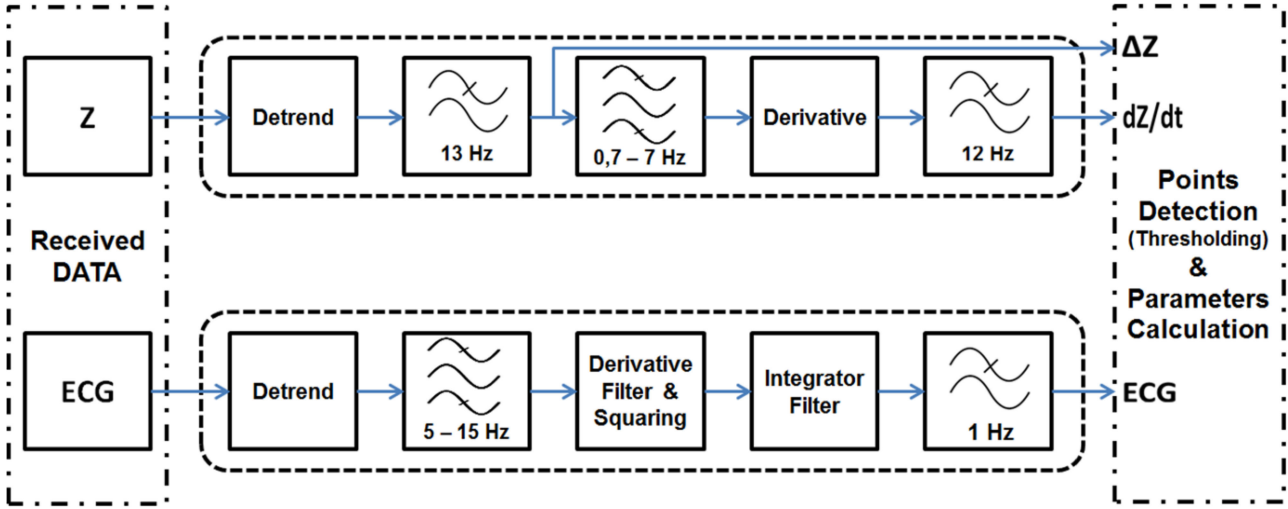


Chart 2. Flow diagram describing the measurement data analysis.

TABLE II  
ICG PARAMETERS

ICG Parameters	Description
Ejection Time ( <i>ET</i> )	Interval time between the X and B points in the $dZ/dt$ in ms.
Pre Ejection Period ( <i>PEP</i> )	Interval time between the B points in the $dZ/dt$ and the Q points in ECG in ms.
Stroke Volume ( <i>SV</i> )	Volume of blood ejected from the left ventricle during one cycle in ml.
Cardiac Output ( <i>CO</i> )	Volume of blood leaving the heart every minute in l/min.
Systolic Time Ratio ( <i>STR</i> )	Coefficient of the temporal distribution between the electrical and the mechanical systole.

results of our algorithm were evaluated with the failure/positive ratio (F/P ratio) previously introduced in [62]. Where terms like failed detection i.e., inaccurate detection, together with false positive, false negative are used, see (4). This ratio indicate the acceptable validity and accuracy of the detection when it is below to 10% [62].

$$\text{Ratio } F/P = \frac{\text{Misdetection} + \text{False positive} + \text{False negative}}{\text{True positive}} \quad (4)$$

- True positive: is the correct detection.
- Misdetection: is the detection of a point that is actually different from the one being evaluated.
- False positive: is an incorrect detection of the point.
- False negative: is completely undetected point.

3) *Signal to Noise Ratio:* The signal to noise ratio (SNR) of both the ICG and ECG signals was evaluated according to (5). To ensure an accurate result of the SNR, the signals used for this calculation were acquired separately, thus, avoiding any

interference of one system with another.

$$SNR = 10\log_{10} \frac{\text{signal power}}{\text{noise power}} \quad (5)$$

For both measured signals, ICG and ECG, the signal power was calculated from the squared RMS amplitude of the non-filtered signal after removing the baseline level. The noise power was calculated using the noise signal acquired and filtering the original signal with a stop band filter applied to the signal frequencies. The baseline was also removed from the noise signal.

## IV. RESULTS

### A. Measurement Instrumentation

A prototype has been designed and implemented and manufactured in house, see Fig. 3 showing the Z-RPI prototype device. The implementation has been executed with 3-stacked printed circuit boards (PCBs) in addition to the battery. The circuitry is contained in a casing of dimensions  $85 \times 56 \times 50$  mm with different functional blocks implemented in each of the 3 stacked boards as showed in Fig. 4.

The management of the measurement system lays in the Raspberry PI3 in the first level on the bottom layer; the measurement operation (MOM) is managed from the Raspberry PI3 together with the wireless communication and the data device's data storage (WDC). The second level hosts the module for conversion and power management (DC/DC, POM), and the third level contains the measurement instrumentation with both is measurement modalities; This level is implemented in a double sided PCB and includes the ECG amplifier (ECG-AFE) and the SoC of the bioimpedance measurement unit, including the AFE module (EBIM), the calibration system module (CSM), and the input/output interface to connect the cables.

The measurement instrumentation allows to record one channel of continuous electrical thoracic bioimpedance and a 3-Lead ECG, with right-leg driven option. The frequency for the bioimpedance measurement is configurable within the range



**Fig. 3.** The Z-RPI device, cables, LiPo battery, power charger and the casing.

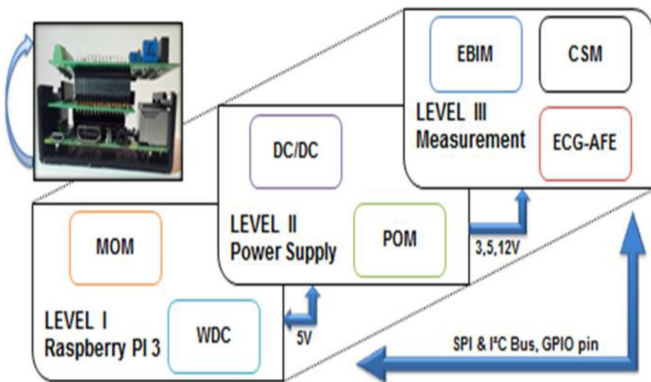


**Fig. 4.** The Z-RPI device 3-level implementation.

**TABLE III**  
MAIN SPECIFICATIONS OF THE Z-RPI

Parameter	Z-RPI
Dimension L × W × H (mm)	85 × 56 × 45
Weight (g)	200
Measurement frequency range (kHz)	1–350
The maximum sampling frequency (Hz)	380
The injecting current ( $\mu$ A)	133, DC free, up till 1 k $\Omega$
Wireless communication	Bluetooth 4.1
Gain	100
CMRR (dB)	110
Electrical patient safety	IEC 6061-1-1, EC 13 and AAMI EC 11

1 kHz to 350 kHz at a sampling rate configurable up to 380 Hz, i.e., it is possible to produce new bioimpedance estimation every 2.6 ms. The ECG recording is sampled at the same sample rate as the ICG recording. The main specifications of the Z-RPI are summarized in **Table III**.

### B. Power Supply

The PowerBoost 1000 charger module has the capacity to recharge a 3.2 V LiPo battery via USB port with 5 V nominal charging voltage. In measurement mode, the LiPo battery provides 3.2 V to the PowerBoost 1000 charger input that boosted up to 5 V in its output which is connected to the +Vcc terminal of the Raspberry PI3. A 3.2 V, 2500 mAh LiPo battery is used to avoid power line connection and making an ambulatory device. The average Z-RPI consumption during the measurement is 440 mA, the Raspberry PI alone in operating mode has 382 mA (370 mA without using Bluetooth) with 127 mA for the standby mode, and the SoC's bloc consume 58 mA (EBIM consume 25 mA, ECG-AFE consume 33 mA). The autonomy of the device measuring continuously is approximately 5 hours with a charging time of 8 h to completely recharge the battery.

### C. ICG Recordings

More than 1500 seconds of recordings were obtained, containing more than 1820 ICG and ECG complexes, similar to the ones plotted in **Fig. 5**, which shows a waveform segment with 3 complexes. **Fig. 5(a)** shows the recording obtained from a volunteer, V1, at 70 kHz, and 257 Hz sampling frequency. **Fig. 5(b)** shows the characteristic waveforms, points and interval times of an ICG/ECG complex.

The average percentage for the Failure/Positive ratio for the B and E points detection was 4.8% with a minimum of 1.2% for volunteer 1 and maximum of 8% for volunteer 4. The average rate for the detection of the X point was 4.5%. With a minimum of 0.9% for volunteer 3 and maximum of 7.3% for volunteer 5.

### D. 3-Lead ECG Recordings

**Fig. 6** shows a 5-second long 3-Lead ECG recordings containing 8 QRS complexes obtained from one volunteers. Lead I is plotted in panel (a), lead II in panel (b) and lead (III) in panel (c).

### E. Signal Characterization

**Table IV** presents descriptive statistics, (mean  $\pm$  SD) for the characterizing parameters and times interval values, calculated from the ICG/ECG recordings obtained for each volunteer.

## V. DISCUSSION

### A. Measurement Instrumentation Settings and Limitations

The purpose of this paper was to describe the development and the implementation of a new affordable and portable instrument for full ICG measurement using Raspberry PI. This new device simultaneously records ECG and ICG signals, sent data via Bluetooth to a PC, where the extraction of the  $\Delta Z$  signal,  $dZ/dt$  signal, ECG signal and the different physiological parameters were calculated using Matlab.

The modular and multilevel concepts as well as the components selected for implementing the Z-RPI are mainly chosen to keep similar dimensions as the Raspberry PI3 in width

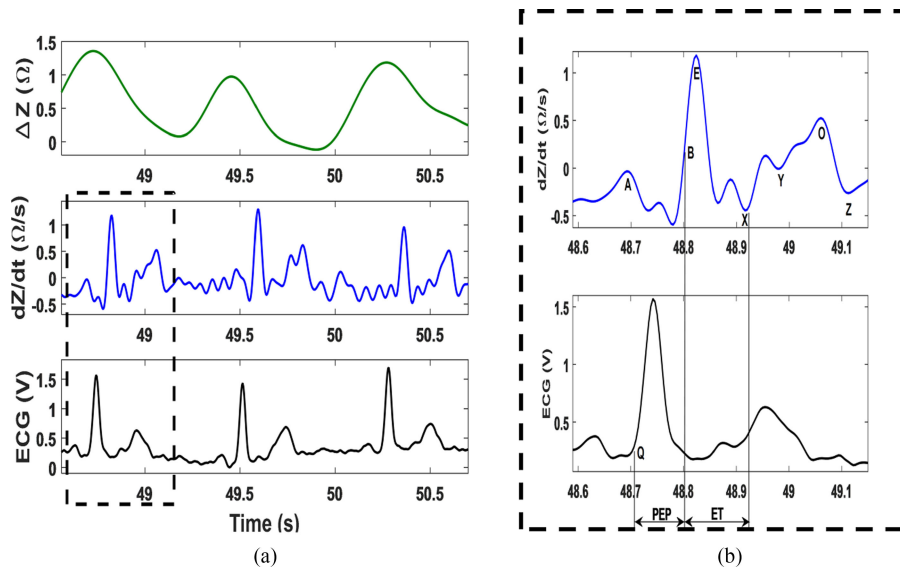


Fig. 5. (a)  $\Delta Z$ ,  $dZ/dt$  and ECG recorded from V1. (b) Point and interval characterizations of V1.

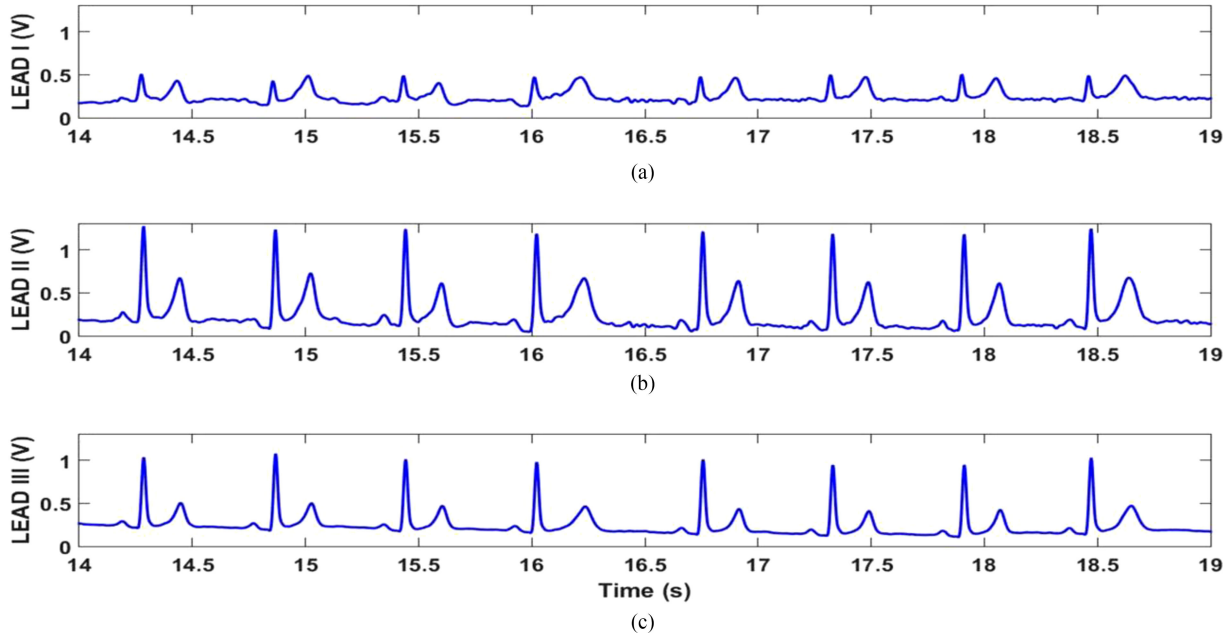


Fig. 6. 3-Lead ECG. (a) Lead I. (b) Lead II. (c) Lead III.

TABLE IV  
PHYSIOLOGICAL PARAMETERS CALCULATED FROM THE SIGNAL ACQUIRED FOR EACH VOLUNTEER

Parameters	V1	V2	V3	V4	V5
$Z_0$ ( $\Omega$ )	$57.6 \pm 4.9$	$45.7 \pm 6.2$	$35.7 \pm 5.6$	$82.2 \pm 1.9$	$68.7 \pm 2.6$
$dZ/dt_{\max}$ ( $\Omega/s$ )	$1.55 \pm 0.22$	$1.19 \pm 0.24$	$1.08 \pm 0.45$	$1.48 \pm 0.18$	$0.91 \pm 0.27$
ET (ms)	$238 \pm 17$	$247 \pm 36$	$290 \pm 71$	$269 \pm 33$	$218 \pm 44$
SV (ml)	$54.3 \pm 5.4$	$48.3 \pm 6.18$	$36.7 \pm 07$	$51 \pm 12.1$	$32.3 \pm 9.2$
CO (l/min)	$4.7 \pm 0.52$	$3.3 \pm 0.3$	$2.4 \pm 0.5$	$2.6 \pm 0.6$	$2.5 \pm 0.5$
PEP (ms)	$146 \pm 34$	$150 \pm 49$	$166 \pm 27$	$197 \pm 60$	$158 \pm 44$
STR	0.61	0.6	0.57	0.76	0.72
HR (bpm)	$87 \pm 4$	$68 \pm 5$	$64 \pm 4$	$50 \pm 4$	$78 \pm 3$
RR (ms)	$691 \pm 33$	$865 \pm 50$	$936 \pm 80$	$1188 \pm 98$	$769 \pm 35$

and length, ensure a reduced weight, meet the requirements for power consumption indicated in Appendix II, and comply with electrical safety guidelines.

In Appendix III, it has been shown that the EBI measurement in the Z-RPI device present a high accuracy to the different impedance measurement at 70 kHz with a maximum error of 1.37% on pure resistors and a maximum error of 2.08% for the 2R1C test. The comparison performed with thoracic measurements against the reference spectrometer SFB7 produced an absolute mean difference for the whole frequency range of 1.57% with a maximum error of 4.55% at 21 kHz. A constant 133  $\mu$ A injecting AC current (DC free) in the range of impedance load from 1  $\Omega$  to 1 k $\Omega$ , a gain of 100 and CMRR of 110 dB, an SNR<sub>Q</sub> equal to 74 dB [63], with a maximum dynamic range of:  $Z_{max} \approx 3.2 \times Z_{calibration}$  and autonomy of 5 hours using wireless communication or more using data storage in the micro SD.

The maximum sampling frequency obtained for the Z-RPI, 380 Hz is good, enough sampling rate for our application: ECG/ICG recordings.

### B. ECG & ICG Measurement Performance

The signal conditioning and pre-processing steps applied to the ICG and ECG recording, allowed us to obtain clean ECG,  $\Delta Z$  and  $dZ/dt$  signals.

The SNR obtained from our experiment for the ECG signal was 90 dB which is near to the maximum values reported by the ADAS1000. Where, according to the ADAS1000 datasheet [51] the maximum signal to noise ratio that is possible to reach is 100 dB, in addition they assume that 100 dB is just in characterization and not in production test [51].

The lower value of SNR in the ICG signal is in general caused by the choice of the excitation current. For several studies that used 2 mA they obtained higher SNR than those with lower current [17], [64]. It is a trade-off since more we manage to have low consumption; the more we get lower SNR. The challenge is to accord the suitable current to obtain a sufficient SNR. In our application, we used a 133  $\mu$ A to have our low battery consumption performance with the SNR obtained for the ICG signal was 53.17 dB, which is sufficient to have a clear signal when the SNR is above 48 dB as reported in [16].

However, the acquired waveforms present a high similarity with the different signals reported in the literature [12], [36], [44].

3-Lead ECG capability allows the systems to be used in applications beyond the typical 3-lead Holter function or heart rate monitoring. To have available both ICG and 3-Lead ECG recordings potentially increases the usefulness of p-health monitoring from mere prompt detection towards early personalized diagnostic applications.

### C. ECG & ICG Characteristic Points & Parameters

The synchronization between the two signals is an important step to perform any accurate assessment of hemodynamics parameters. In our case it was performed by taking into consid-

eration the information on the ADAS1000 and AD5933 signal acquisition pathway time, 2 ms and 1.9 ms respectively, according to the datasheets [43], [51], and the difference time between the acquisition of the ECG and ICG value, 2 ms, due to the sequential process of data storage implemented in the firmware of the Z-RPI. In addition, the delay caused by the digital filters used in the analysis on Matlab software were also estimated by using the grpdelay function of Matlab that was estimated at 19 samples (74 ms) for the ECG and 12 samples (47 ms) for the ICG. All of these times were considered during the digital signal processing and the remaining delay between the ECG and ICG recording was cancelled.

Comparing the average F/P ratio value of 3.8% reported in [62] for the E wave detection with 4.8 and 4.5% values obtained in this work, suggests a similar performance regarding the detection of the main characteristic points of in the ICG complex.

From the hemodynamic parameters calculated from the ICG recordings, the value for the PEP reported for volunteer 4, 197 ms, is slightly higher than the rest and might be outside the expected variation for PEP value in humans [12], [17], [65].

The value of PEP obtained may differ due to the method used to calculate [61]. It is a fact that using signal averaging would decrease the variability of the PEP as well as the rest of parameters values converging the values to more standard values [12], [65]. The obtained 197 ms value has been obtained without signal averaging, when the ensemble averaging method was applied like [65]–[68] the PEP value obtained for volunteer 4 decreased from 197 ms to 145 ms, which is a value completely within normal range(50–150 ms) [12], [17].

## VI. CONCLUSION & FUTURE WORK

This study has been designed from an educational and quick prototyping perspective, focusing mainly in measurement performance, and therefore lacks the work required to assess its suitability for clinical purposes. Further experimentation towards clinical validation should be done to be able to address any potential use in p-health applications.

After the evaluation, the obtained recordings, the calculated hemodynamic parameters and considering the fulfillment of the technical specification in Appendix II, we find the performance of the implemented system, Z-RPI satisfactory for the intended purpose of this development.

The evaluation results show that the new affordable instrument developed with Raspberry PI3 functions effectively and accurately and has successfully shown that developments with EBI technology can also benefit from Raspberry PI community for engineering educational purposes and research applications.

Using sensorized garments with integrated textile electrodes [17], [36], placed thorax region and incorporating the signal processing on the Raspberry PI configured in Bluetooth Low Energy mode to transfer the calculated values is a potential perspective toward enabling applications of Z-RPI for wearable and p-health monitoring applications.

**TABLE V**  
LOAD DYNAMIC TEST RANGE

fm = 70 kHz	Theoretical ( $\Omega$ )	Mean measured ( $\Omega$ )	Error ( $\Omega$ )	Abs. Error (%)
R	24	23,67	0,33	1,37
	50	50,6	0,6	1,20
	75	74,16	0,84	1,12
	100	99,86	0,14	0,14
	130	128,63	1,37	1,05
	150	151,92	1,92	1,28
	175	172,7	2,3	1,31

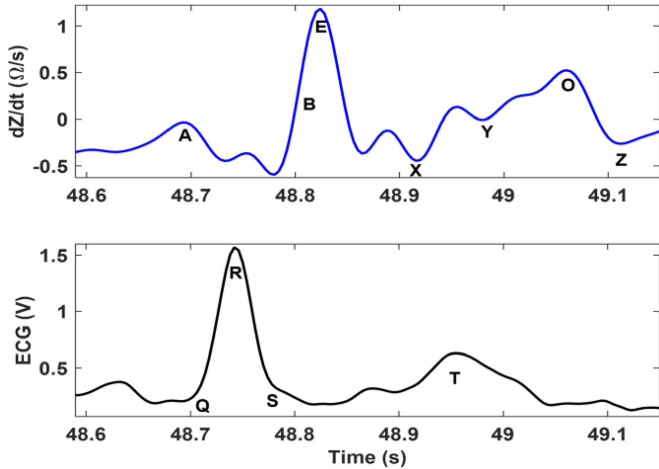


**Fig. 7.** Typical ICG waveform and their characteristics points.

#### APPENDIX I IMPEDANCE CARDIOGRAPHY. PRINCIPLES AND APPLICATIONS

Impedance Cardiography (ICG) uses electrical bioimpedance to describe the mechanical function of the heart. Using a 4-electrode technique, current is injected through the thorax region and the resulting voltage is acquired. Thus, using the law of Ohm, the impedance is obtained. The measured impedance contains changes caused by the blood flowing from the heart, aorta and other major vessels in the thorax and it is noted as  $\Delta Z$ .

The derivative ( $dZ/dt$ ) of the  $\Delta Z$  is characterized by seven typical characteristic points which are related to cardiodynamics [12], [57]. A (atrial contraction), B (aortic valve opening) it occurs on the ascending part of the E point, E (the maximum aortic flow) defined as the maximum point on the  $dZ/dt$  waveform (noted  $dZ/dt_{max}$ ), X (aortic valve closing) which is the minimum notch after the E point, Y (the pulmonic valve closing), O (mitral valve opening), Z (mitral regurgitation) it is described as a decreasing after the O point.

These characteristic points are used to calculate certain hemodynamic parameters and time intervals that have a direct description of the mechanical function of the heart [11]–[13], [69]. Those parameters are: cardiac output (CO) and stroke volume (SV). And the time intervals are: left ventricular ejection time (ET), Pre-ejection period (PEP), systolic time ratio (STR).

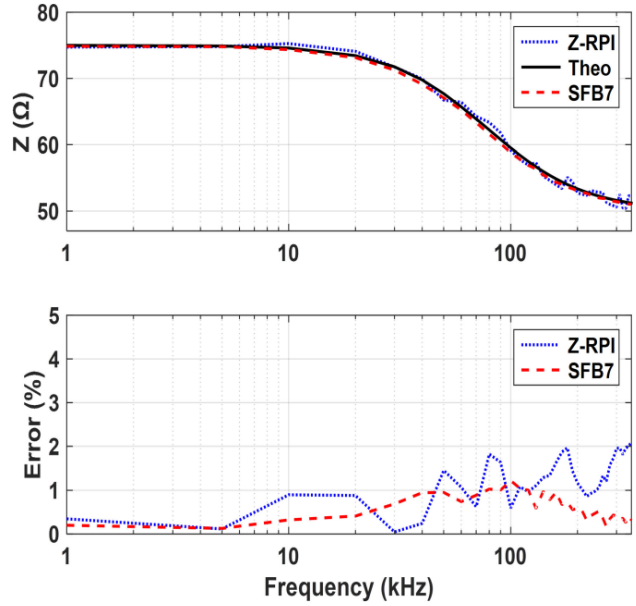


**Fig. 8.** Spectroscopy impedance measurement of the 2R1C system and its error: Theoretical value (line trace); Z-RPI measurement (dot point trace); SFB7 measurement (dashed trace).

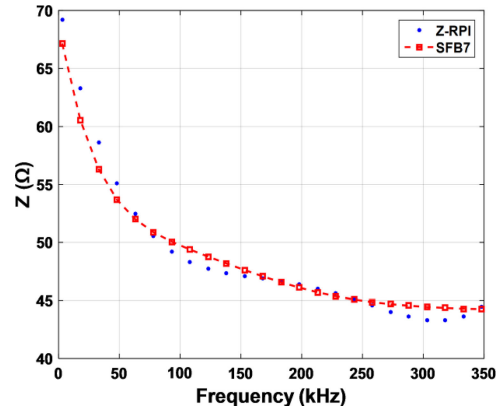


**Fig. 9.** Mean Thoracic spectroscopy bioimpedance spectra obtained from 10 continuous measurements taken in 20 s: Z-RPI measurement (dotted trace); SFB7 measurement (dashed trace).

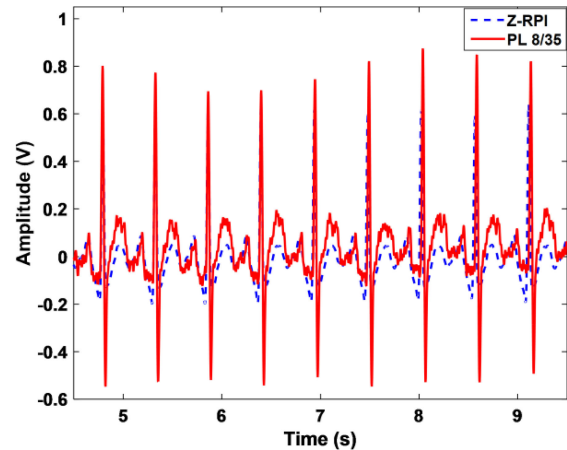


**Fig. 10.** ECG measurements: Z-RPI measurement (dashed trace) (with mean RR = 0.54 s  $\pm$  0.008, and HR = 111 b/m); Powerlab 8/35 measurement (line trace) (with mean RR = 0.55 s  $\pm$  0.02, and HR = 109 b/m).

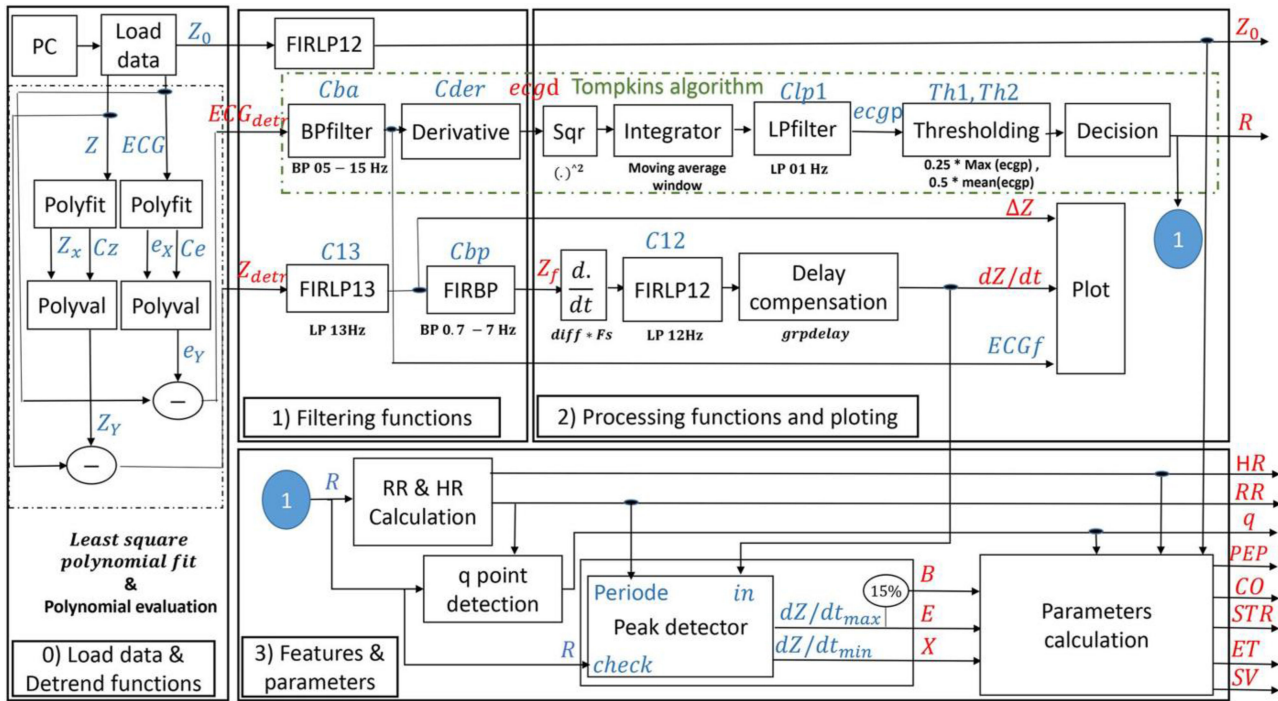


Fig. 11. Functional chart of the customize program running MATLAB.

The CO shows the working capacity of the heart and the cardiovascular system. The systolic time intervals show a direct relation with the cardiac systole. The calculation of the CO requires other hemodynamic indices such as SV that is also related to the systolic time indices such as ET [70].

## APPENDIX II TARGETED TECHNICAL SPECIFICATIONS

The performed work has been executed targeting the following specifications:

- Perform a 3-lead ECG measurement.
- Perform a 4-electrode Impedance Cardiography with a impedance measurement error  $<3\%$  [71], [72].
- Perform single and multi-frequency impedance measurement.
- Minimum sampling frequency  $\geq 250$  Hz.
- Battery capacity for over 4 hours of continuous recordings.
- Wireless capabilities communication.
- For impedance measurement:  $\text{SNR}_Q > 59$  dB, and  $\text{SNR} > 46$  dB [16].
- CMRR over 80 dB for frequency up till 100 kHz.

## APPENDIX III MEASUREMENT PERFORMANCE AND CIRCUIT VERIFICATION

The performance evaluation of our system included, a comparison measurement with a reference bioimpedance spectrometer, the SFB7 (Impedimed, Brisbane). Both in electrical circuit models and in-vivo. For all measurements, the system was calibrated in multipoint mode using a resistor of  $100 \Omega$  1% and

the measurement error of the modulus of the impedance was calculated.

The measurements in circuits contained:

- A spectroscopy impedance measurement over a 2R1C impedance system,
- A single frequency, dynamic load test resistance measurement for frequency,  $f_m = 70$  kHz, and value range from  $24 \Omega$  to  $175 \Omega$ .
- A bioimpedance spectroscopy measurement ranging from 1 kHz to 350 kHz over the thorax.

In addition, a simultaneous comparison recording for the ECG measurement was done with the Z-RPI and the reference instrument Powerlab 8/35 (ADIstruments Pty Ltd) for the lead II with using the same electrodes, and the same filters for both signal recorded.

The obtained performance is presented in Table V and plots in Figs. 8–10.

## APPENDIX IV CUSTOMIZE PROGRAM RUNNING MATLAB

The software in the computer execute the following tasks: Data loading, Detrending, Filtering, HR detection and parameter calculation. The specific functions are outlined in detailed in the functional chart depicted in Fig. 11.

## ACKNOWLEDGMENT

The authors would like to thank the research group Textile and Wearable Sensing for p-Health Solutions, University of Borås.

## REFERENCES

- [1] World Health Organization, "Cardiovascular diseases (CVDs)," *Media Centre*, World Health Organization, Geneva, Switzerland, 2016.
- [2] S. Said and G. T. Hernandez, "The link between chronic kidney disease and cardiovascular disease," *J. Nephropathol.*, vol. 3, pp. 99–104, 2014.
- [3] U. G. Kyle *et al.*, "Bioelectrical impedance analysis—part I: Review of principles and methods," *Clin. Nutrition*, vol. 23, pp. 1226–1243, 2004.
- [4] S. B. Heymsfield, D. Gallagher, J. Grammes, C. Nuñez, Z. Wang, and A. Pietrobelli, "Upper extremity skeletal muscle mass: potential of measurement with single frequency bioimpedance analysis," *Appl. Radiat. Isotopes*, vol. 49, pp. 473–474, 1998.
- [5] J. C. Marquez, F. Seoane, E. Välimäki, and K. Lindecrantz, "Comparison of dry-textile electrodes for electrical bioimpedance spectroscopy measurements," *Proc. J. Phys., Conf. Ser.*, vol. 224, 2010, Art. no. 012140.
- [6] Y. Yamamoto, T. Nakamura, and T. Kusuhara, "Consideration of conditions required for multi-channel simultaneous bioimpedance measurement," in *Proc. IEEE Conf. Instrum. Meas. Technol.*, 1998, pp. 231–234.
- [7] N. Van Helleputte *et al.*, "A 345  $\mu$ W multi-sensor biomedical SoC with bio-impedance, 3-channel ECG, motion artifact reduction, and integrated DSP," *IEEE J. Solid-State Circuits*, vol. 50, no. 1, pp. 230–244, Jan. 2015.
- [8] R. V. Davalos, D. M. Otten, L. M. Mir, and B. Rubinsky, "Electrical impedance tomography for imaging tissue electroporation," *IEEE Trans. Biomed. Eng.*, vol. 51, no. 5, pp. 761–767, May 2004.
- [9] J. Nyboer, M. M. Kreider, and L. Hannapel, "Electrical impedance plethysmography," *Circulation*, vol. 2, pp. 811–821, 1950.
- [10] J. Miller and S. Horvath, "Impedance cardiography," *Psychophysiology*, vol. 15, pp. 80–91, 1978.
- [11] M. T. Allen, J. Fahrenberg, R. M. Kelsey, W. R. Lovallo, and L. J. Doornen, "Methodological guidelines for impedance cardiography," *Psychophysiology*, vol. 27, pp. 1–23, 1990.
- [12] G. Cybulski, "Ambulatory impedance cardiography," in *Ambulatory Impedance Cardiography*. New York, NY, USA: Springer, 2011, pp. 39–56.
- [13] D. P. Bernstein, I. C. Henry, M. J. Banet, and T. Dittrich, "Stroke volume obtained by electrical interrogation of the brachial artery: transbrachial electrical bioimpedance velocimetry," *Physiol. Meas.*, vol. 33, pp. 629–649, 2012.
- [14] Centers For Medicare & Medicaid Services, "National Coverage Determination (NCD) for cardiac output monitoring by Thoracic Electrical Bioimpedance (TEB). In:(DHS) DoHHS," *Dept. Health Human Serv., Centers Med. Medicaid Serv.*, Baltimore, MD, USA, 2006.
- [15] H. Woltjer, B. J. van der Meer, H. Bogaard, and P. M. de Vries, "Comparison between spot and band electrodes and between two equations for calculations of stroke volume by means of impedance cardiography," *Med. Biol. Eng. Comput.*, vol. 33, pp. 330–334, 1995.
- [16] H. Yazdanian, A. Mahnam, M. Edrisi, and M. A. Esfahani, "Design and implementation of a portable impedance cardiography system for noninvasive stroke volume monitoring," *J. Med. Signals Sensors*, vol. 6, pp. 47–56, 2016.
- [17] M. Ulbrich, *Non-Invasive Stroke Volume Assessment Using the Thoracic Electrical Bioimpedance: Advances in Impedance Cardiography*. Aachen, Germany: Shaker Verlag, 2016.
- [18] C. N. Beccetti, Gamma Cardio CG, Rome, Italy. [Online]. Available: <http://www.gammacardiosoft.it/>. Accessed on: Nov. 2016.
- [19] F. Abtahi, J. Snäll, B. Aslamy, S. Abtahi, F. Seoane, and K. Lindecrantz, "Biosignal pi, an affordable open-source ECG and respiration measurement system," *Sensors*, vol. 15, pp. 93–109, 2015.
- [20] S. Patel, H. Park, P. Bonato, L. Chan, and M. Rodgers, "A review of wearable sensors and systems with application in rehabilitation," *J. Neuroeng. Rehabil.*, vol. 9, 2012, Art. no. 21.
- [21] Y.-L. Zheng *et al.*, "Unobtrusive sensing and wearable devices for health informatics," *IEEE Trans. Biomed. Eng.*, vol. 61, no. 5, pp. 1538–1554, May 2014.
- [22] X.-F. Teng, Y.-T. Zhang, C. C. Poon, and P. Bonato, "Wearable medical systems for p-health," *IEEE Rev. Biomed. Eng.*, vol. 1, pp. 62–74, 2008.
- [23] B. Antonescu and S. Basagni, "Wireless body area networks: challenges, trends and emerging technologies," in *Proc. 8th Int. Conf. Body Area Netw.*, 2013, pp. 1–7.
- [24] N. Meziane, J. Webster, M. Attari, and A. Nimunkar, "Dry electrodes for electrocardiography," *Physiol. Meas.*, vol. 34, pp. R47–R69, 2013.
- [25] N. Meziane, S. Yang, M. Shokoueinejad, J. Webster, M. Attari, and H. Eren, "Simultaneous comparison of 1 gel with 4 dry electrode types for electrocardiography," *Physiol. Meas.*, vol. 36, pp. 513–529, 2015.
- [26] R. Harder, A. Diedrich, J. S. Whitfield, M. S. Buchowski, J. B. Pietsch, and F. J. Baudenbacher, "Smart multi-frequency bioelectrical impedance spectrometer for BIA and BIVA applications," *IEEE Trans. Biomed. Circuits Syst.*, vol. 10, no. 4, pp. 912–919, Aug. 2016.
- [27] B. Zhou *et al.*, "A Bluetooth low energy approach for monitoring electrocardiography and respiration," in *Proc. IEEE 15th Int. Conf. e-Health Netw., Appl. Serv.*, 2013, pp. 130–134.
- [28] R. Kusche, S. Kaufmann, and M. Ryschka, "Design, development and comparison of two different measurement devices for time-resolved determination of phase shifts of bioimpedances," in *Proc. 3rd Student Conf. Med. Eng. Sci.*, 2014, pp. 115–119.
- [29] F. Abtahi, B. Aslamy, I. Boujabir, F. Seoane, and K. Lindecrantz, "An affordable ECG and respiration monitoring system based on raspberry PI and ADAS1000: First step towards homecare applications," in *Proc. 16th Nordic-Baltic Conf. Biomed. Eng.*, 2015, pp. 5–8.
- [30] V. Pockevicius, V. Markevicius, M. Cepenas, D. Andriukaitis, and D. Navikas, "Blood glucose level estimation using interdigital electrodes," *Elektronika Ir Elektrotehnika*, vol. 19, pp. 71–74, 2013.
- [31] Y. Zhang and C. Harrison, "Tomo: Wearable, low-cost electrical impedance tomography for hand gesture recognition," in *Proc. 28th Annu. ACM Symp. User Interface Softw. Technol.*, 2015, pp. 167–173.
- [32] S. Weyer, T. Menden, L. Leicht, S. Leonhardt, and T. Wartzek, "Development of a wearable multi-frequency impedance cardiography device," *J. Med. Eng. Technol.*, vol. 39, pp. 131–137, 2015.
- [33] X. Hu, X. Chen, R. Ren, B. Zhou, Y. Qian, and H. Li, "Portable health monitoring device for electrocardiogram and impedance cardiography based on bluetooth low energy," *J. Fiber Bioeng. Informat.*, vol. 7, pp. 397–408, 2014.
- [34] M. Ulbrich *et al.*, "The IMPACT shirt: textile integrated and portable impedance cardiography," *Physiol. Meas.*, vol. 35, pp. 1181–1196, 2014.
- [35] M. J. Liebo, R. P. Katra, N. Chakravarthy, I. Libbus, and W. W. Tang, "Non-invasive wireless bioimpedance monitoring tracks patients with healthcare utilization following discharge from acute decompensated heart failure: Results from the ACUTE pilot study," *J. Cardiac Failure*, vol. 19, pp. S88–S89, 2013.
- [36] J. C. M. Ruiz, M. Remppfer, F. Seoane, and K. Lindecrantz, "Textrode-enabled transthoracic electrical bioimpedance measurements—towards wearable applications of impedance cardiography," *J. Elect. Bioimpedance*, vol. 4, pp. 45–50, 2013.
- [37] J. Ferreira, I. Pau, K. Lindecrantz, and F. Seoane, "A handheld and textile-enabled bioimpedance system for ubiquitous body composition analysis. An initial functional validation," *IEEE J. Biomed. Health Informat.*, vol. 21, no. 5, pp. 1224–1232, Sep. 2017.
- [38] M. Ulbrich, J. Mühlsteff, H. Reiter, C. Meyer, and S. Leonhardt, "Wearable solutions using bioimpedance for cardiac monitoring," in *Recent Advances in Ambient Assisted Living-Bridging Assistive Technologies, E-Health and Personalized Health Care*, vol. 20. Amsterdam, The Netherlands: IOS Press, 2015, pp. 30–44.
- [39] R. Roy and K. Venkatasubramanian, "EKG/ECG based driver alert system for long haul drive," *Indian J. Sci. Technol.*, vol. 8, no. 19, pp. 1–6, 2015.
- [40] F. Mocq, Raspberry Pi 3 ou Pi Zero Exploitez tout le potentiel de votre nano-ordinateur, Edition ENI, 2016, 850 pages.
- [41] R. P. Foundation, "Raspberry Pi 3 Model B." [Online]. Available: <https://www.raspberrypi.org/products/raspberry-pi-3-model-b/>. Accessed on: Aug. 2016.
- [42] M. McCauley, "C library for Broadcom BCM 2835 as used in Raspberry Pi," BCM2835, 2013. [Online]. Available: <http://www.airspayce.com/mikem/bcm2835/index.html>
- [43] Analog Devices, Norwood, MA, USA, "AD5933 datasheet," 2007.
- [44] J. Ferreira, F. Seoane, and K. Lindecrantz, "Portable bioimpedance monitor evaluation for continuous impedance measurements. Towards wearable plethysmography applications," in *Proc. 35th Annu. Int. Conf. IEEE Eng. Med. Biol. Soc.*, 2013, pp. 559–562.
- [45] J. Ferreira, F. Seoane, and K. Lindecrantz, "AD5933-based electrical bioimpedance spectrometer. Towards textile-enabled applications," in *Proc. Annu. Int. Conf. IEEE Eng. Med. Biol. Soc.*, 2011, pp. 3282–3285.
- [46] F. Seoane, J. Ferreira, J. J. Sanchéz, and R. Bragós, "An analog front-end enables electrical impedance spectroscopy system on-chip for biomedical applications," *Physiol. Meas.*, vol. 29, pp. S267–S267, 2008.
- [47] U. Pliquet and A. Barthel, "Interfacing the AD5933 for bio-impedance measurements with front ends providing galvanostatic or potentiostatic excitation," in *Proc. J. Phys., Conf. Ser.*, 2012, Paper 012019.
- [48] V. V. Tsibulko, I. T. Iliev, and I. I. Jekova, "Methods for detecting pacemaker pulses in ECG signal: A review," *Annu. J. Electron.*, vol. 8, pp. 77–80, 2014.

- [49] D. Vasava and S. Deshpande, "Portable health monitoring device," *Int. J. Eng. Res. Gen. Sci.*, vol. 4, no. 3, pp. 807–812, 2016.
- [50] I. Korsakov, S. Kuptsov, D. Raznometov, V. Feklistov, and M. Sumskoy, "Prototype X73-PHD 3-lead ECG device for personal healthcare1," *Egyptian Comput. Sci. J.*, vol. 37, no. 7, pp. 51–61, 2013.
- [51] Analog Devices, Norwood, MA, USA, "Low power five electrode electrocardiogram (ECG) analog front end," *ADAS1000 Datasheet*, 2012.
- [52] Analog Devices, Norwood, MA, USA, "ADG774 Datasheet."
- [53] A. Huang and L. Rudolph, *Bluetooth for Programmers*. Cambridge, MA, USA: Massachusetts Inst. Technol., 2005.
- [54] J. Pan and W. J. Tompkins, "A real-time QRS detection algorithm," *IEEE Trans. Biomed. Eng.*, vol. BME-32, no. 3, pp. 230–236, Mar. 1985.
- [55] R. van Lien, N. M. Schutte, J. H. Meijer, and E. J. de Geus, "Estimated preejection period (PEP) based on the detection of the R-wave and dZ/dt-min peaks does not adequately reflect the actual PEP across a wide range of laboratory and ambulatory conditions," *Int. J. Psychophysiol.*, vol. 87, pp. 60–69, 2013.
- [56] W. Kubicek *et al.*, "The Minnesota impedance cardiograph-theory and applications," *Biomed. Eng.*, vol. 9, pp. 410–416, 1974.
- [57] Z. Lababidi, D. Ehmke, R. E. Durnin, P. E. Leaverton, and R. M. Lauer, "The first derivative thoracic impedance cardiogram," *Circulation*, vol. 41, pp. 651–658, 1970.
- [58] K. Sakamoto, K. Muto, H. Kanai, and M. Iizuka, "Problems of impedance cardiography," *Med. Biol. Eng. Comput.*, vol. 17, pp. 697–709, 1979.
- [59] M. Ulbrich, J. Mühlsteff, S. Leonhardt, and M. Walter, "Influence of physiological sources on the impedance cardiogram analyzed using 4D FEM simulations," *Physiol. Meas.*, vol. 35, pp. 1451–1468, 2014.
- [60] M. Ulbrich, J. Mühlsteff, P. Paluchowski, and S. Leonhardt, "Erythrocyte orientation and lung conductivity analysis with a high temporal resolution FEM model for bioimpedance measurements," in *Lecture Notes on Impedance Spectroscopy: Measurement, Modeling and Applications*, vol. 3. Boca Raton, FL, USA: CRC Press, 2012, p. 71.
- [61] P. Carvalho, R. P. Paiva, J. Henriques, M. Antunes, I. Quintal, and J. Mühlsteff, "Robust characteristic points for ICG-definition and comparative analysis," in *Proc. BIOSIGNALS*, 2011, pp. 161–168.
- [62] M. Rempfler, "On the feasibility of textrodes for impedance cardiography," *Biomed. Eng.*, thesis no. 1, 2011, 66 pages.
- [63] Analog Devices, Norwood, MA, USA, "AD5933, MSPS, 12 bit impedance converter network analyzer, preliminary technical data," 2007.
- [64] N. C. S. Capela, "Impedance cardiography," M.S. thesis, Univ. Coimbra, Coimbra, Portugal, 2013.
- [65] H. Riese *et al.*, "Large-scale ensemble averaging of ambulatory impedance cardiograms," *Behav. Res. Methods*, vol. 35, pp. 467–477, 2003.
- [66] Y. Miyamoto, M. Takahashi, T. Tamura, T. Nakamura, T. Hiura, and M. Mikami, "Continuous determination of cardiac output during exercise by the use of impedance plethysmography," *Med. Biol. Eng. Comput.*, vol. 19, pp. 638–644, 1981.
- [67] M. Muzy, D. C. Jeutter, and J. J. Smith, "Computer-automated impedance-derived cardiac indexes," *IEEE Trans. Biomed. Eng.*, vol. BME-33, no. 1, pp. 42–47, Jan. 1986.
- [68] R. M. Kelsey and W. Guethlein, "An evaluation of the ensemble averaged impedance cardiogram," *Psychophysiology*, vol. 27, pp. 24–33, 1990.
- [69] W. Kubicek, R. Patterson, and D. Witsoe, "Impedance cardiography as a noninvasive method of monitoring cardiac function and other parameters of the cardiovascular system," *Ann. New York Acad. Sci.*, vol. 170, pp. 724–732, 1970.
- [70] D. Bernstein and H. Lemmens, "Stroke volume equation for impedance cardiography," *Med. Biol. Eng. Comput.*, vol. 43, pp. 443–450, 2005.
- [71] A. Piccoli, G. Pastori, M. Guizzo, M. Rebeschini, A. Naso, and C. Cascone, "Equivalence of information from single versus multiple frequency bioimpedance vector analysis in hemodialysis," *Kidney Int.*, vol. 67, pp. 301–313, 2005.
- [72] C. P. Earthman, R. R. Wolfe, and S. B. Heymsfield, "Dudrick Research Symposium 2015—lean tissue and protein in health and disease: Key targets and assessment strategies," *J. Parenteral Enteral Nutrition*, vol. 41, pp. 226–237, 2017.